Control of Nonlinear Dynamical Systems Modeled by Recurrent Neural Networks

Michael Nikolaou and Vijaykumar Hanagandi
Dept. of Chemical Engineering, Texas A&M University, College Station, TX 77843

Process modeling with recurrent neural networks has been shown to be a successful methodology for the modeling of systems whose internal structure may not be well known. You and Nikolaou (1993) showed that recurrent neural networks can effectively model nonlinear single-input-single-output (SISO) or multiple-input-multiple-output (MIMO) systems, in batch or continuous mode of operation, based on exact or noisy data. As will be shown in the sequel, an additional advantage of using RNNs for plant modeling is that, because of their form, RNNs are directly amenable to manipulations for controller design through exact linearization (EL) (Isidori and Ruberti, 1984; Kravaris and Chung, 1987).

EL can be applied directly to nonlinear systems of the form:

$$\frac{dx}{dt}=f[x(t)]+g[x(t)]u(t), \quad x(t)\in\mathbf{R}^n, \quad u(t)\in\mathbf{R}^m \tag{1}$$

$$y(t)=h[x(t)], \quad y(t)\in\mathbf{R}^m \tag{2}$$

For systems of the form:

$$\frac{dx}{dt}=f[x(t), u(t)], \quad x(t)\in\mathbf{R}^n, \quad u(t)\in\mathbf{R}^m \tag{3}$$

$$y(t)=h[x(t), u(t)], \quad y(t)\in\mathbf{R}^m \tag{4}$$

a direct (but somewhat impractical) approach appeared in Li and Feng (1987), and an indirect method is discussed in Nijmeijer and van der Schaft (1990).

Use of RNNs for dynamical plant identification and controller design has the following characteristics:

- An RNN does not require any *a priori* internal understanding of the plant or any *linearity* assumptions. On the other hand, for successful modeling more data must be available to offset the lack of internal (first principle) system understanding.
- An RNN approximates plant dynamics through adjustment of the number of hidden nodes and the values of weights. Thus, selecting a model structure is equivalent to simply changing the number of hidden nodes. The real states of the plant are not necessary.
- Determining the values of internal weights, referred to as training of the RNN, is a particular form of nonlinear regression, for which effective distributed algorithms are available (Almeida, 1989; Pearlmutter, 1989; Williams and Zipser, 1989; You and Nikolaou, 1993). Newton-like algorithms can also be used. It should be stressed that the approximation capabilities of the RNN are limited by the number of training sets available.

The plant modeling and controller design methodology proposed here comprise three steps:

- Model the nonlinear plant using an RNN.
- Exact-linearize the nonlinear RNN.
- Design a linear controller for the exact-linearized model, and implement it on the real plant.

Exact Linearization Background

We will consider, for simplicity, SISO systems ($m=1$ in Eqs. 1 and 2). For MIMO systems, refer to Isidori and Ruberti (1984) or Kravaris and Soroush (1990).

The stable SISO nonlinear system P modeled by Eqs. 1 and 2 is *exact-linearizable*, if there exists a positive integer r, called the *exact linearizability index* or *relative order* of P, such that:

$$L_gL_f^{r-1}h(x)\neq 0 \tag{5}$$

where the above Lie derivative $L_gL_f^{r-1}h(x)$ is defined by the equations:

$$L_fh:=\langle dh, f\rangle:=\nabla_fh:=\frac{\partial h}{\partial x}f:=\sum_{i=1}^{n}\frac{\partial h}{\partial x_i}f_i,$$

$$L_f^rh:=\underbrace{L_fL_f\ldots L_fh}_{r \text{ times}}$$

If $r<\infty$, then the state feedback,

$$u=\frac{v-\sum_{k=0}^{r}\beta_kL_f^kh(x)}{\beta_rL_gL_f^{r-1}h(x)}, \tag{6}$$

Correspondence concerning this article should be addressed to M. Nikolaou.

creates a linear system L between the new input v and the original output y, described by the equation:

$$\sum_{k=0}^{r} \beta_k \frac{d^k y}{dt^k} = v \tag{7}$$

where β_k are selected so that the poles of the resultant linear system are in desired locations of the complex plane.

The states x of the nonlinear system P are often not available. If the process is open-loop stable, an open-loop nonlinear observer can be used to reconstruct x. The EL then corresponds to feedforward EL through system inversion (Hirschorn, 1979). Indeed, we have $Pu = y = Lv \Rightarrow u = P^{-1}Lv$.

Recurrent Neural Networks Background

RNNs can be traced back to the work of McCulloch and Pitts (1943). Without loss of generality we will consider here a SISO RNN (Figure 1). A node's input-output dynamics are dictated by the differential equation:

$$\frac{dx_i}{dt} = -\frac{x_i}{T_i} + (1-\delta_{i,I})\frac{F(\Sigma_j w_{ij}x_j)}{T_i} + \delta_{i,I}\frac{U}{T_i}, \quad i = 1, \ldots, n \tag{8}$$

where I refers to the input node, $\delta_{ij} = 1$ if $i = j$, else 0; x_i is the ith node output, $i = 1, \ldots, n$; w_{ij} is the connection weight from the jth node to the ith node; U is the external input; T_i is the time constant associated with the ith node; and $F(x) = 1/(1 + e^{-x})$ is the squashing function for each hidden node.

Main Result

For a SISO system with one input (node 2), one output (node 3), one bias (node 1), and $(n-3)$ hidden nodes, Eq. 8 can be written explicitly as:

$$\begin{bmatrix} \frac{dx_1}{dt} \\ \frac{dx_2}{dt} \\ \frac{dx_3}{dt} \\ \vdots \\ \frac{dx_n}{dt} \end{bmatrix} = \begin{bmatrix} 0 \\ -\frac{x_2(t)}{T_2} \\ -\frac{x_3(t)}{T_3} + \frac{F[\Sigma_j w_{3j}x_j(t)]}{T_3} \\ \vdots \\ -\frac{x_n(t)}{T_n} + \frac{F[\Sigma_j w_{nj}x_j(t)]}{T_n} \end{bmatrix} + \begin{bmatrix} 0 \\ \frac{1}{T_2} \\ 0 \\ \vdots \\ 0 \end{bmatrix} U \tag{9}$$

Comparing Eq. 9 to Eqs. 1 and 2 it is clear that an RNN is directly amenable to exact linearization. It is straightforward to show that for such a system the linearizability index r satisfies the inequality $r \geq 2$. For $r = 2$, the input and state transformation $\Omega(v, x)$ has the form:

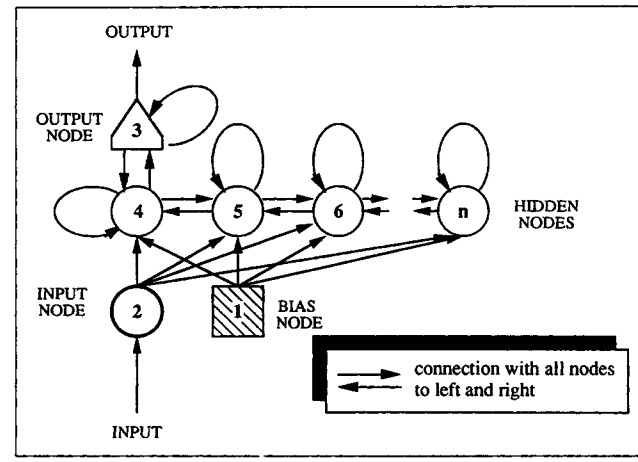

Figure 1. General configuration of a recurrent neural network.

$$u = \frac{v - \left(\beta_0 x_3 + \beta_1 f_3 + \beta_2 \sum_{i=1}^{n} f_i \frac{\partial f_3}{\partial x_i}\right)}{\frac{1}{T_2}\beta_2 \frac{\partial f_3}{\partial x_2}}$$

If the inverse of the mapping P: $u \to y$ is stable (in the sense of Nikolaou and Manousiouthakis, 1989), then exact linearization yields a stable linear mapping L: $v \to y$ (by appropriate selection of β_i) and a stable *nonlinear* mapping $V = P^{-1}L$: $v \to u$ (Nikolaou and Manousiouthakis, 1990). In that case, a controller can be designed for the transfer function,

$$L(s) = \frac{y(s)}{v(s)} = \frac{1}{\beta_0 + \beta_1 s + \ldots + \beta_r s^r}$$

according to any linear controller design technique. If P^{-1} is unstable, then no general methodology exists for the design of an optimal controller, for example, in a worst-case setting such as the linear H_∞ case. An optimal controller can be designed for a particular set-point change, such as a step (Wright and Kravaris, 1992).

Modeling Uncertainty

Let P_m be a model for the real plant P. If P_m^{-1} is stable and L is designed to be stable, then the real operator between v and y resulting from EL, is $PP_m^{-1}L$, since the output y_m of the model P_m is:

$$y_m = Lv = P_m u \Rightarrow u = P_m^{-1}Lv \Rightarrow y = Pu = PP_m^{-1}Lv.$$

Let $\Delta L = PP_m^{-1}L - L$ and $\|P - P_m\| \leq \delta$, where $\|N\|$ denotes the induced norm of an unbiased nonlinear operator N over a set U, defined as:

$$\|N\| = \sup_{u \in U} \frac{\|Nu\|}{\|N\|}.$$

Then,

$$\|\Delta L\| = \|PP_m^{-1}L - L\| = \|PP_m^{-1}L - P_mP_m^{-1}L\|$$
$$= \|(P-P_m)P_m^{-1}L\| \le \|P-P_m\|\,\|P_m^{-1}L\| \le \delta\|P_m^{-1}L\|$$

The above inequality provides a modeling error, based on which linear robust controller design may be attempted. Calculation of the number δ is a formidable problem, addressed by Nikolaou and Manousiouthakis (1989).

Case Study

We chose a nonisothermal continuous stirred tank reactor (CSTR), because of its nonlinearity. CSTR's real behavior is assumed to be represented by the following equations (Stephanopoulos, 1984):

$$\frac{dC_A}{dt} = \frac{F_I}{V}[C_{AI} - C_A(t)] - kC_A(t)\exp\left(-\frac{E}{RT}\right) \quad (12)$$

$$\frac{dT}{dt} = \frac{F_I}{V}[T_I - T(t)] - \frac{\Delta H_R}{\rho C_P}kC_A(t)\exp\left(-\frac{E}{RT}\right) - \frac{Q(t)}{\rho C_P V} \quad (13)$$

where C_A is the concentration of species A in the reactor; T is the temperature [output $y = (T - T_s)/T_s$]; and Q is the heat removal rate [input $u = (Q - Q_s)/Q_s$]. Parameter values are shown below.

F_I (m³/h)	V (m³)	C_{AI} (mol/m³)	k (1/h)	E/R (K)	ΔH_R (J/mol)	T_I (K)	ρ (kg/m³)	C_P (J/kg·K)
1.133	1.36	8,008	7.08×10^7	8,375	−69,775	373.3	800.8	3,140

An RNN (with one input, one bias, and six hidden nodes) was trained with simulated training data obtained from Eqs. 12 and 13 (Sarimveis, 1992). Since the states of that RNN are artifacts and do not correspond to measurable quantities, the trained RNN was used as an open-loop observer to provide the RNN states to the block Ω. For the resulting exact-linearized system,

$$L(s) = \frac{1}{\beta_0 + \beta_1 s + \beta_2 s^2} \quad (\beta_0 = \beta_1 = \beta_2 = 1),$$

the PID controller,

$$C(s) = \frac{\beta_1}{\epsilon}\left(1 + \frac{\beta_0}{\beta_1 s} + \frac{\beta_2}{\beta_1}s\right) \quad (\epsilon = 1),$$

is optimal (Morari and Zafiriou, 1990) resulting in the closed-loop transfer function,

$$\frac{y(s)}{y^{SP}(s)} = \frac{1}{\epsilon s + 1} \text{ (independent of } \beta_i).$$

The overall feedback loop is depicted in Figure 2. For comparison, a linear IMC controller was designed for the linear CSTR model obtained through Taylor series linearization

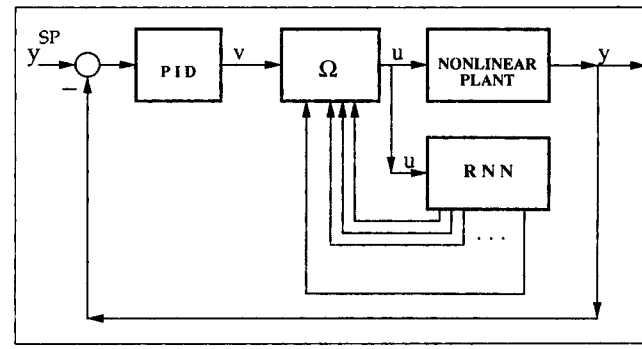

Figure 2. RNN-based feedback loop.

around the steady state (C_{As}, T_s, U_s) = (393.3 mol/m³, 547.556 K, 1.055×10^8 J/h). The same closed-loop transfer function,

$$\frac{y(s)}{y^{SP}(s)} = \frac{1}{\epsilon s + 1},$$

was used in this design.

Results and Discussion

Figure 3 shows responses of the system's temperature T to step changes on the setpoint T^{SP} at $t = 10$ h, for both linear and nonlinear controller designs. It is evident that there are set-point changes (for example, 8.7%) for which the controller

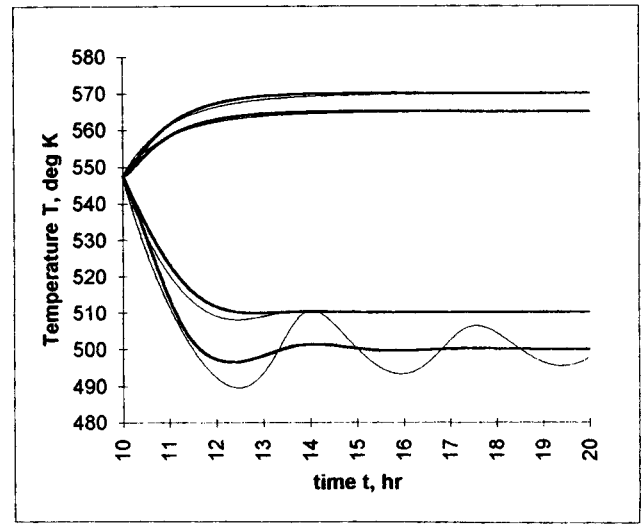

Figure 3. Closed-loop responses of CSTR to various set-point changes.

Bold and thin lines indicate RNN-based and linear control loop responses, respectively.

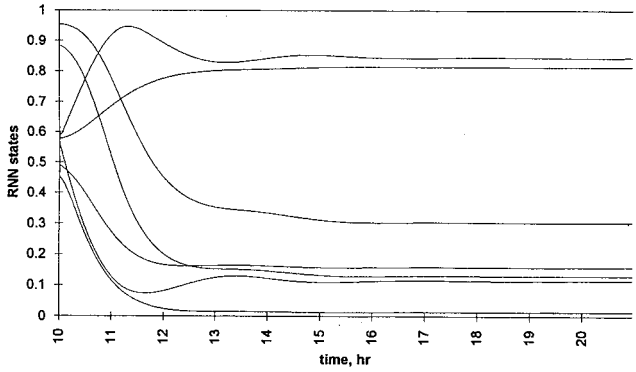

Figure 4. Response of RNN states for setpoint change $T^{SP} = 500$ K.

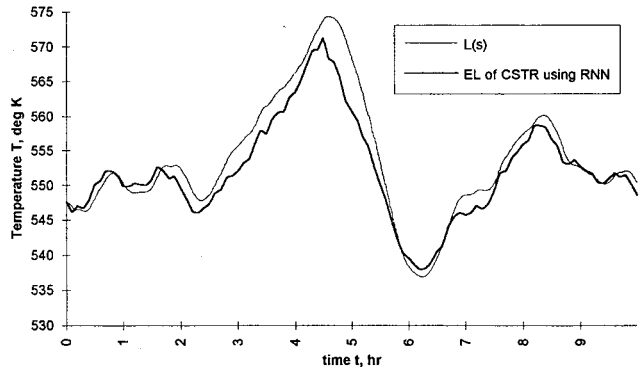

Figure 6. Comparison between the responses of the transfer function $1/(1+s+s^2)$ and the exact-linearized CSTR to v, with v taking random values in $[-2, 2]$.

of Figure 2 performs clearly better than the corresponding linear controller. The following remarks are in order:

• Figure 3 shows that for the nonlinear controller design the mapping $T^{SP} \rightarrow T$ approaches the linear transfer function $1/(s+1)$. A small discrepancy is due to the fact that the RNN only approximates the first-principles CSTR model. Good closed-loop performance in the presence of this plant/model mismatch is the evidence, albeit not the proof, of robustness of the proposed nonlinear controller.

• The eigenvalues of $\{A_{ij}\} = \{(\partial f_i/\partial x_j)_{(U_s,x_s)}\}$, listed below, guarantee local stability of the observer.

-0.844	-1.06	-1.15	-1.55	-1.88	$-3.47+2.76i$	$-3.47-2.76i$

Figure 4 shows responses of the RNN states for the setpoint change $T^{SP} = 500$ K (Figure 3).

• The zeros of the transfer function $[(x-x_s)(s)]/[(U-U_s)(s)]$, listed below, show that P^{-1} is locally stable, implying that the mapping between v and u is locally stable.

$-1.60+1.02i$	$-1.60-1.02i$	-9.21	-1.81	-1.44

Figure 5 shows u to be bounded and within feasible bounds for the setpoint change $T^{SP} = 500$ K (Figure 3).

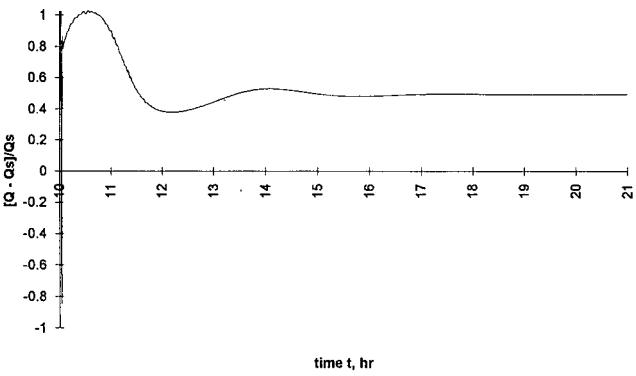

Figure 5. RNN-based controller output for setpoint change $T^{SP} = 500$ K.

• The responses of the transfer function, $1/(\beta_o+\beta_1 s+\beta_2 s^2)$, and the exact-linearized CSTR to v, with v taking random values in $[-2, 2]$, are compared in Figure 6. The discrepancy is due to the approximation of CSTR dynamics by the RNN.

• Small perturbations to the values of the CSTR parameters resulted in no appreciable deterioration of performance. For example, 40 h after a setpoint change to 500 K, T_I and F_I were changed from 8,008 mol/m^3 and 1.133 m^3/h to 7,800 mol/m^3 and 1.0 m^3/h, respectively. The behavior of the closed-loop CSTR is shown in Figure 7. The superiority of the RNN-based controller is clear.

Conclusions

An integrated methodology was presented, for the modeling and controller design of nonlinear dynamical systems. The methodology, which comprises three steps, was tested on a CSTR and shown to perform better than a linear, optimally-tuned controller. A number of theoretical issues remain to be investigated, most notably robust stability and performance.

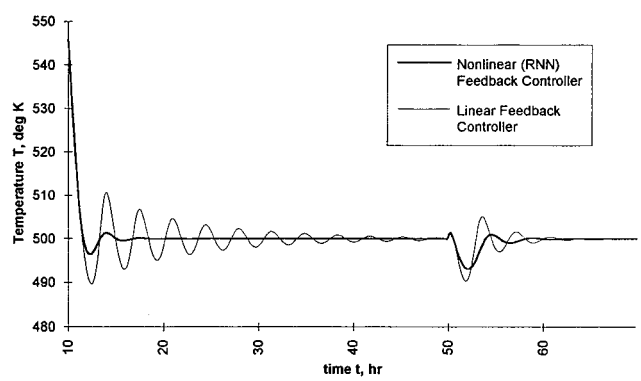

Figure 7. Rejection of disturbances at $t = 50$ h by RNN-based and linear control loops.

The multivariable case will be presented in a forthcoming publication.

Acknowledgment

Financial support from the National Science Foundation through a Research Initiation Grant (CTS-9009376) is gratefully acknowledged.

Literature Cited

Almeida, L. B., "Back-Propagation in Non-Feedforward Networks," *Neural Computing Architectures*, I. Aleksander, ed., MIT Press, Cambridge, MA (1989).

Hirschorn, R. M., "Invertibility of Multivariable Nonlinear Control Systems," *IEEE Trans. AC*, **AC-24**(6), 855 (1979).

Isidori, A., *Nonlinear Control Systems: An Introduction*, 2nd ed., Springer-Verlag (1989).

Isidori, A., and A. Ruberti, "On the Synthesis of Linear Input-Output Responses for Nonlinear Systems," *Sys. and Control Lett.*, **4**, 17 (1984).

Kravaris, C., and C. B. Chung, "Nonlinear State Feedback Synthesis by Global Input/Output Linearization," *AIChE J.*, **33**, 592 (1987).

Kravaris, C., and M. Soroush, "Synthesis of Multivariable Nonlinear Controllers by Input/Output Linearization," *AIChE J.*, **36**, 249 (1990).

Li, C. W., and Y. K. Feng, "Functional Reproducibility of General Multivariable Analytic Non-linear Systems," *Int. J. Control.*, **45**, 255 (1987).

McCulloch, W. S., and W. Pitts, "A Logical Calculus of the Ideas Immanent in Nervous Activity," *Bull. of Math. Biophys.*, **5**, 115 (1943).

Morari, M., and E. Zafiriou, *Robust Process Control*, Prentice-Hall, Englewood Cliffs, NJ (1990).

Nijmeijer, H., and A. J. van der Schaft, *Nonlinear Dynamical Control Systems*, Springer-Verlag (1990).

Nikolaou, M., and A. Manousiouthakis, "Stability Aspects of Exact Linearization Methods: A Hybrid Approach," *Proc. Amer. Control Conf.*, San Diego, CA, p. 2736 (1990).

Nikolaou, M., and V. Manousiouthakis, "A Hybrid Approach to Nonlinear System Stability and Performance," *AIChE J.*, **35**, 559 (1989).

Pearlmutter, B. A., "Learning State Space Trajectories in Recurrent Networks," *Proc. IJCNN*, Washington, DC, p. 2 (1989).

Sarimveis, H., "Artificial Neural Networks for Input-Output Dynamic Modeling of Nonlinear Processes," MS Thesis, Texas A&M Univ. (1992).

Stephanopoulos, G., *Chemical Process Control: An Introduction to Theory and Practice*, Prentice-Hall, Englewood Cliffs, NJ (1984).

Williams, R. J., and D. Zipser, "A Learning Algorithm for Continually Running Fully Recurrent Neural Networks," *Neural Comp.*, **1**, 270 (1989).

Wright, R. A., and C. Kravaris, "Nonminimum-Phase Compensation for Nonlinear Processes," *AIChE J.*, **38**, 26 (1992).

You, Y., and M. Nikolaou, "Dynamic Process Modeling with Recurrent Neural Networks," *AIChE J.*, **39**, 1654 (1993).